ON THE KHOVANOV AND KNOT FLOER HOMOLOGIES OF QUASI-ALTERNATING LINKS

CIPRIAN MANOLESCU AND PETER OZSVÁTH

Abstract. Quasi-alternating links are a natural generalization of alternating links. In this paper, we show that quasi-alternating links are "homologically thin" for both Khovanov homology and knot Floer homology. In particular, their bigraded homology groups are determined by the signature of the link, together with the Euler characteristic of the respective homology (i.e. the Jones or the Alexander polynomial). The proofs use the exact triangles relating the homology of a link with the homologies of its two resolutions at a crossing.

1. Introduction

In recent years, two homological invariants for oriented links $L \subset S^3$ have been studied extensively: Khovanov homology and knot Floer homology. Our purpose here is to calculate these invariants for the class of quasi-alternating links introduced in [19], which generalize alternating links.

The first link invariant we will consider in this paper is *Khovanov's reduced homology* ([5],[6]). This invariant takes the form of a bigraded vector space over $\mathbb{Z}/2\mathbb{Z}$, denoted $\widetilde{Kh}^{i,j}(L)$, whose Euler characteristic is the Jones polynomial in the following sense:

$$\sum_{i\in\mathbb{Z},j\in\mathbb{Z}+\frac{l-1}{2}} (-1)^i q^j \text{rank } \widetilde{Kh}^{i,j}(L) = V_L(q),$$

where l is the number of components of L. The indices i and j are called the homological and the Jones grading, respectively. (In our convention j is actually half the integral grading j from [5].) The indices appear as superscripts because Khovanov's theory is conventionally defined to be a cohomology theory. It is also useful to consider a third grading δ, described by the relation $\delta = j - i$.

Khovanov's original definition gives a theory whose Euler characteristic is the Jones polynomial multiplied by the factor $q^{1/2} + q^{-1/2}$; for the reduced theory, the Euler characteristic is the usual Jones polynomial, i.e. normalized so that it takes the value 1 on the unknot, cf. [6]. Note that $\widetilde{Kh}$ can be also be defined with integer coefficients, but then it depends on the choice of a component of the link.

The other homological link invariant that we consider in this paper is *knot Floer homology*. This theory was independently introduced by Szabó and the second author in [15], and by Rasmussen [27]. In its simplest form, it is a bigraded Abelian group $\widehat{HFK}_i(L,j)$ whose Euler characteristic is (up to a factor) the Alexander-Conway polynomial $\Delta_L(q)$:

$$\sum_{j\in\mathbb{Z},i\in\mathbb{Z}+\frac{l-1}{2}} (-1)^{i+\frac{l-1}{2}} q^j \text{rank } \widehat{HFK}_i(L,j) = (q^{-1/2} - q^{1/2})^{l-1} \cdot \Delta_L(q).$$

CM was supported by a Clay Research Fellowship.

PSO was supported by NSF grant numbers DMS-0505811 and FRG-0244663.

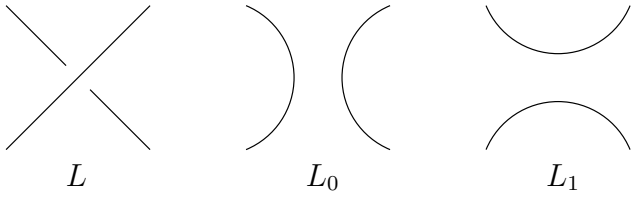

FIGURE 1. The links in the unoriented skein relation.

Knot Floer homology was originally defined using pseudo-holomorphic curves, but there are now also several combinatorial formulations available, cf. [10], [11], [29], [24]. The two gradings i and j are called the *Maslov* and *Alexander gradings* respectively; we also set $\delta = j - i$ as above. Knot Floer homology detects the genus of a knot [17], as well as whether a knot is fibered [25]. There exists also an improvement, called link Floer homology ([22], [23]), which detects the Thurston norm of the link complement, but that theory will not be discussed in this paper. Also, even though $\widehat{HFK}$ can be defined with integer coefficients, in this paper we will only consider it with coefficinets in the field $\mathbb{F} = \mathbb{Z}/2\mathbb{Z}$.

For many classes of links (including most knots with small crossing number), the Khovanov and knot Floer homologies over $R = \mathbb{Z}$ or $\mathbb{F}$ take a particularly simple form: they are free R-modules supported in only one δ-grading. We call such links *Khovanov homologically thin (over R)*, or *Floer homologically thin (over R)*, depending on which theory we refer to. Various versions of these definitions appeared in [2], [27], [6], [28]. Further, it turns out that typically the δ-grading in which the homology groups are supported equals $-\sigma/2$, where σ is the signature of the link. When this is the case, we say that the link is (Khovanov or Floer) *homologically σ-thin*. (Floer homologically σ-thin knots were called *perfect* in [26].)

If a link L is homologically σ-thin over $R = \mathbb{Z}$ or $\mathbb{F}$ for a bigraded theory $\mathcal{H}$ (where $\mathcal{H}$ could denote either $\widetilde{Kh}$ or $\widehat{HFK}$), then $\mathcal{H}(L)$ is completely determined by the signature σ of L and the Euler characteristic $P(q)$ of $\mathcal{H}$ (the latter being either the Jones or a multiple of the Alexander polynomial). Indeed, if $P(q) = \sum a_j q^j$, we must have:

$$\mathcal{H}^{i,j}(L) \simeq \begin{cases} R^{|a_j|} & \text{if } i = j + \frac{\sigma}{2} \\ 0 & \text{otherwise.} \end{cases}$$

In the world of Khovanov homology, the fact that the vast majority (238) of the 250 prime knots with up to 10 crossings are homologically σ-thin was first observed by Bar-Natan, based on his calculations in [2]. Lee [7] showed that alternating links are Khovanov homologically σ-thin. Since 197 of the prime knots with up to 10 crossings are alternating, this provides a partial explanation for Bar-Natan's observation.

At roughly the same time, a similar story unfolded for knot Floer homology. Rasmussen [26] showed that 2-bridge knots are Floer homologically σ-thin; and this result was generalized in [16] to all alternating knots.

In this paper we generalize these results to a larger class of links, the *quasi-alternating links* of [19]. Precisely, $\mathcal{Q}$ is the smallest set of links satisfying the following properties:

- The unknot is in $\mathcal{Q}$;
- If L is a link which admits a projection with a crossing such that
  (1) both resolutions L_0 and L_1 at that crossing (as in Figure 1) are in $\mathcal{Q}$,
  (2) $\det(L) = \det(L_0) + \det(L_1)$,
  then L is in $\mathcal{Q}$.

The elements of $\mathcal{Q}$ are called quasi-alternating links. It it is easy to see (cf. [19, Lemma 3.2]) that alternating links are quasi-alternating.

In this paper we prove the following:

Theorem 1. *Quasi-alternating links are Khovanov homologically σ-thin (over $\mathbb{Z}$).*

Theorem 2. *Quasi-alternating links are Floer homologically σ-thin (over $\mathbb{Z}/2\mathbb{Z}$).*

For knots with up to nine crossings, Theorem 1 and Theorem 2 provide a complete explanation for the prevalence of homological σ-thinness (over the respective coefficient ring). Indeed, among the 85 prime knots with up to nine crossings, only two (8_{19} and 9_{42}) are not Khovanov homologically σ-thin, and these are also the only ones which are not Floer homologically σ-thin. By the results of [19], [9] and [1], all 83 of the remaining knots are quasi-alternating. (Among them, 74 are alternating.)

Unfortunately, in general it is difficult to decide whether a larger, homologically σ-thin knot is quasi-alternating. In fact, it remains a challenge to find homologically σ-thin knots that are not quasi-alternating.

A few words are in order about the strategy of proof and the organization of the paper. Both Theorem 1 and Theorem 2 are consequences of the unoriented skein exact triangles satisfied by the respective theories. For Khovanov homology, this exact triangle (which relates the homology of L to that of its resolutions L_0 and L_1, cf. Figure 1), is immediate from the definition of the homology groups. The only new ingredient used in the proof of Theorem 1 is an observation about relating the gradings to the signature. We explain this in Section 2 of the paper. In fact, the proof of Theorem 1 is an adaptation of the proof of the corresponding fact for alternating links due to Lee [7].

For knot Floer homology, an unoriented skein exact triangle was described by the first author in [9]. In that paper, the maps in the triangle were ungraded. In Section 3, we show that they actually respect the δ-grading, up to a well-determined shift. This will imply Theorem 2. It is interesting to note that this strategy is quite different from the earlier proofs for two-bridge and alternating links, [27], [16].

We remark that Theorem 2 has a number of formal consequences. The full version of knot Floer homology is a graded, filtered chain complex over the polynomial algebra $\mathbb{F}[U]$. It was shown in [16, Theorem 1.4 and the remark immediately after] that for Floer homologically σ-thin knots, their full complex (up to equivalence) is determined by their Alexander polynomial and signature. Theorem 2 implies then that this is true for quasi-alternating knots. Furthermore, according to [20] and [21], the full knot Floer complex has enough information to determine the Heegaard Floer homology of any Dehn surgery on that knot. Thus, the Floer homologies (over $\mathbb{F}$) of Dehn surgeries on quasi-alternating knots are determined by the Alexander polynomial, the signature, and the surgery coefficient; we refer to [16], [20], [21] for the precise statements.

It is natural to expect Theorem 2 to hold also over $\mathbb{Z}$. Note that Theorem 2, combined with the universal coefficients theorem, implies that quasi-alternating links are Floer homologically σ-thin over $\mathbb{Q}$.

Acknowledgments. We would like to thank John Baldwin, Matthew Hedden, Robert Lipshitz, Jacob Rasmussen and Sucharit Sarkar for helpful conversations.

2. The exact triangle for Khovanov homology

2.1. **The Gordon-Litherland formula.** Let us review the definition of the Goeritz matrix, as well as the Gordon-Litherland formula for the signature, following [3].

FIGURE 2. Incidence numbers and types of crossings.

Consider an oriented link L in S^3 with a regular, planar projection, and let D be the corresponding planar diagram. The complement of the projection in $\mathbb{R}^2$ has a number of connected components, which we call *regions*. We color them in black and white in checkerboard fashion. Let $R_0, R_1, \dots, R_n$ be the white regions. Assume that each crossing is incident to two distinct white regions. To each crossing c we assign an incidence number $\mu(c)$, as well as a type (I or II), as in Figure 2. Note that the sign of the crossing is determined by its incidence number and type.

Set

$$\mu(D) = \sum_{c \text{ of type II}} \mu(c).$$

The Goeritz matrix $G = G(D)$ of the diagram D is defined as follows. For any $i, j \in \{0, 1, \dots, n\}$ with $i \neq j$, let

$$g_{ij} = -\sum_{c \in \bar{R}_i \cap \bar{R}_j} \mu(c).$$

Set also

$$g_{ii} = -\sum_{i \neq j} g_{ij}.$$

Then G is the $n \times n$ symmetric matrix with entries g_{ij}, for $i, j \in \{1, \dots, n\}$.

Gordon and Litherland showed that the signature of L is given by the formula

$$\sigma(L) = \text{signature}(G) - \mu(D). \tag{1}$$

(We use the convention that the signature of the right-handed trefoil is -2.) Also, the determinant $\det(L)$ of a link L can be defined as the non-negative integer

$$\det(L) = |\det(G)|.$$

2.2. **The signature of resolutions.** Let $L \subset S^3$ be an oriented link with a fixed planar projection as before. Fix now a crossing c_0 in the corresponding planar diagram. If the crossing is positive (resp. negative), we set $L_+ = L$ (resp. $L_- = L$) and let L_- (resp. L_+) be the link obtained form L by changing the sign of the crossing. Further, we denote by L_v and L_h the oriented and unoriented resolutions of L at that crossing, cf. Figure 3. (We choose an arbitrary orientation for L_h.) To make the connection with Figure 1, note that if $L = L_+$, then $L_0 = L_v$ and $L_1 = L_h$, while if $L = L_-$, then $L_0 = L_h$ and $L_1 = L_v$.

Denote by D_+, D_v, D_h the planar diagrams of L_+, L_v, L_h, respectively, differing from each other only at the chosen crossing c_0.

The first equality in the lemma below (without the sign) is due to Murasugi [12]; the second is also inspired by a result of Murasugi from [13].

Lemma 3. *Suppose that* $\det(L_v), \det(L_h) > 0$ *and* $\det(L_+) = \det(L_v) + \det(L_h)$. *Then:*

$$\sigma(L_v) - \sigma(L_+) = 1$$

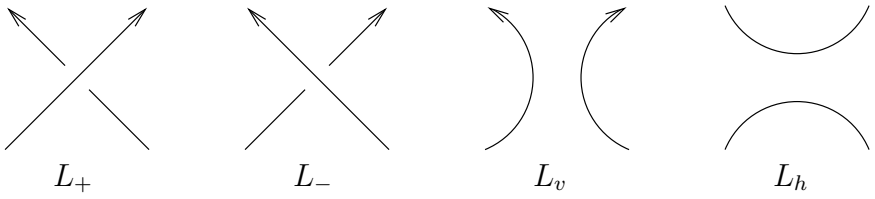

FIGURE 3. Two possible crossings and their resolutions.

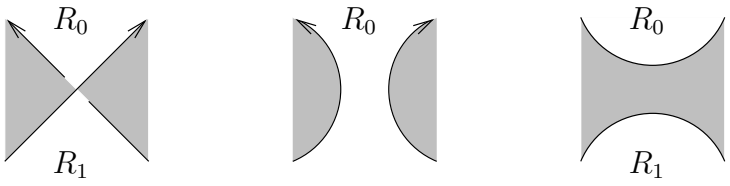

FIGURE 4. Coloring convention at the chosen crossing.

and

$$\sigma(L_h) - \sigma(L_+) = e,$$

where e denotes the difference between the number of negative crossings in D_h and the number of such crossings in D_+.

Proof. Construct the Goeritz matrices $G_+ = G(D_+), G_v = G(D_v)$ and $G_h = G(D_h)$ in such a way that c_0 is of Type I (and incidence number -1) in D_+, and the white region R_0 (the one not appearing in the Goeritz matrix) is as in Figure 4.

Observe now that G_+ and G_h are bordered matrices of G_v. More precisely, if G_v is an $n \times n$ symmetric matrix, then there exists $a \in \mathbb{R}$ and $v = (v_1, \dots, v_n) \in \mathbb{R}^n$ such that

$$G_+ = \begin{pmatrix} a & v \\ v^T & G_v \end{pmatrix}; \quad G_h = \begin{pmatrix} a+1 & v \\ v^T & G_v \end{pmatrix}.$$

Without loss of generality (after an orthonormal change of basis), we can assume that G_v is diagonal, with diagonal entries $\alpha_1, \dots, \alpha_n$. Note that these are nonzero because $\det(L_v) = |\det(G_v)| \neq 0$.

The bilinear form associated to G_+ can be written as

$$aX^2 + 2\sum_{i=1}^{n} v_i X X_i + \sum_{i=1}^{n} \alpha_i X_i^2,$$

or

$$\Big(a - \sum_{i=1}^{n} \frac{v_i^2}{\alpha_i}\Big)X^2 + \sum_{i=1}^{n} \alpha_i \Big(X_i + \frac{v_i}{\alpha_i} X\Big)^2.$$

A similar formula holds for the form of G_h, but with a replaced by $a+1$.

If we set

$$\beta = a - \sum_{i=1}^{n} \frac{v_i^2}{\alpha_i},$$

then

$$\det(G_+) = \beta \cdot \det(G_v), \quad \det(G_h) = (\beta + 1) \cdot \det(G_v).$$

By the condition on the determinants in the hypothesis, $|\beta| = |\beta+1|+1$, so we must have $\beta < -1$. Therefore, when we diagonalize the bilinear forms, for G_+ (resp. G_h) we get one additional negative coefficient (β, resp. $\beta+1$) as compared to G_v. Thus,

$$\text{signature}(G_+) = \text{signature}(G_h) = \text{signature}(G_v) - 1. \tag{2}$$

Since c_0 is of Type I, we also have $\mu(D_+) = \mu(D_v)$. Together with the Gordon-Litherland formula (1), these identities imply

$$\sigma(L_+) = \sigma(L_v) - 1.$$

Next, observe that when we change the direction of an arc at a crossing, both the sign and the type of the crossing are reversed, but the incidence number remains the same. If we denote by $k(\mu, t)$ the number of crossings of incidence number $\mu \in \{\pm 1\}$ and type $t \in \{I, II\}$ in D_+ (excluding c_0) which change type (and sign) in D_h, then

$$\mu(D_h) - \mu(D_+) = k(+1, I) - k(-1, I) - k(+1, II) + k(-1, II).$$

This equals

$$-\big(k(-1, I) + k(+1, II)\big) + \big(k(+1, I) + k(-1, II)\big) = -e.$$

Using (1) and (2) again, we get

$$\sigma(L_+) = \sigma(L_h) + e,$$

as desired. □

2.3. **An unoriented skein exact triangle.** The following proposition is a simple consequence of the definition of Khovanov cohomology. It is implicit in [5], and also appeared in Viro's work [30]. The statement below, with the precise gradings, is taken from Rasmussen's review [28, Proposition 4.2]. It is written there in terms of Khovanov's unreduced homology, but it works just as well for the reduced version $\widetilde{Kh}$, which we use in this paper. We work over $\mathbb{Z}$, so to define the reduced homology we need to mark a component for each link appearing in the triangle; we do this by marking the same point on their diagrams, away from the crossing where the links differ.

Proposition 4. *(Khovanov, Viro, Rasmussen) There are long exact sequences*

$$\cdots \to \widetilde{Kh}^{i-e-1, j-\frac{3e}{2}-1}(L_h) \to \widetilde{Kh}^{i,j}(L_+) \to \widetilde{Kh}^{i, j-\frac{1}{2}}(L_v) \to \widetilde{Kh}^{i-e, j-\frac{3e}{2}-1}(L_h) \to \cdots$$

and

$$\cdots \to \widetilde{Kh}^{i, j+\frac{1}{2}}(L_v) \to \widetilde{Kh}^{i,j}(L_-) \to \widetilde{Kh}^{i-e+1, j-\frac{3e}{2}+1}(L_h) \to \widetilde{Kh}^{i+1, j+\frac{1}{2}}(L_v) \to \cdots$$

where e is as in the statement of Lemma 3.

If we forget about i and j and just keep the grading $\delta = j - i$, the two triangles become

$$\cdots \to \widetilde{Kh}^{*-\frac{e}{2}}(L_h) \to \widetilde{Kh}^{*}(L_+) \to \widetilde{Kh}^{*-\frac{1}{2}}(L_v) \to \widetilde{Kh}^{*-\frac{e}{2}-1}(L_h) \to \cdots \tag{3}$$

and

$$\cdots \to \widetilde{Kh}^{*+\frac{1}{2}}(L_v) \to \widetilde{Kh}^{*}(L_-) \to \widetilde{Kh}^{*-\frac{e}{2}}(L_h) \to \widetilde{Kh}^{*-\frac{1}{2}}(L_v) \to \cdots \tag{4}$$

Proposition 5. *Let L be a link and L_0, L_1 its two resolutions at a crossing as in Figure 1. Assume that* $\det(L_0), \det(L_1) > 0$ *and* $\det(L) = \det(L_0) + \det(L_1)$. *Then there is an exact triangle:*

$$\cdots \to \widetilde{Kh}^{*-\frac{\sigma(L_1)}{2}}(L_1) \to \widetilde{Kh}^{*-\frac{\sigma(L)}{2}}(L) \to \widetilde{Kh}^{*-\frac{\sigma(L_0)}{2}}(L_0) \to \widetilde{Kh}^{*-\frac{\sigma(L_1)}{2}-1}(L_1) \to \cdots$$

Proof. When the given crossing in L is positive, this is a re-writing of the triangle (3), taking into account the result of Lemma 3. Note that when following three consecutive maps in the triangle the grading decreases by one; thus, the grading change for the map between the homologies of the two resolutions is determined by the grading change for the other two maps.

The case when the crossing is negative is similar. □

Proof of Theorem 1. Note that any quasi-alternating link has nonzero determinant; this follows easily from the definition. The desired result is then a consequence of Proposition 5: the unknot is homologically σ-thin and, because of the exact triangle, if L_0 and L_1 are homologically σ-thin, then so is L. □

3. The exact triangle for knot Floer homology

In this section we assume that the reader is familiar with the basics of knot Floer homology (including the version with several basepoints), cf. [15], [27], [22], [10]. Throughout this section we will work with coefficients in the field $\mathbb{F} = \mathbb{Z}/2\mathbb{Z}$.

3.1. **Heegaard diagrams and periodic domains.** We start with a few generalities about periodic domains in Heegaard diagrams. Our discussion is very similar to the ones in [18, Section 2.4] and [22, Section 3.4], except that here we do not ask for the periodic domains to avoid any basepoints.

Let Σ be a Riemann surface of genus g. A collection $\boldsymbol{\alpha} = (\alpha_1, \dots, \alpha_n)$ of disjoint, simple closed curves on Σ is called *good* if the span S_α of the classes $[\alpha_i]$ in $H_1(\Sigma; \mathbb{Z})$ is g-dimensional. If $\boldsymbol{\alpha}$ is such a collection, we view (the closures of) the components of $\Sigma - (\cup \alpha_i)$ as two-chains on Σ and denote by Π_α their span. Note that Π_α is a free Abelian group of rank $m = n - g + 1$.

A *Heegaard diagram* $(\Sigma, \boldsymbol{\alpha}, \boldsymbol{\beta})$ consists of a Riemann surface Σ together with two good collections of curves $\boldsymbol{\alpha} = (\alpha_1, \dots, \alpha_n)$ and $\boldsymbol{\beta} = (\beta_1, \dots, \beta_n)$. (A Heegaard diagram describes a 3-manifold Y; see for example [22, Section 3.1].) We define a *periodic domain* in the Heegaard diagram $(\Sigma, \boldsymbol{\alpha}, \boldsymbol{\beta})$ to be a two-chain on Σ that is a linear combination of the components of $\Sigma - (\cup \alpha_i) - (\cup \beta_i)$, and with the property that its boundary is a linear combination of the alpha and beta curves. (This is a slight modification of [18, Definition 2.14].) The group of periodic domains is denoted $\Pi_{\alpha,\beta}$. Let also $S_{\alpha,\beta} = S_\alpha + S_\beta$ be the span of all the alpha and beta curves in $H_1(\Sigma; \mathbb{Z})$.

Lemma 6. *The group $\Pi_{\alpha,\beta}$ of periodic domains is free Abelian of rank equal to $2n + 1 - \operatorname{rank}(S_{\alpha,\beta})$.*

Proof. There is a map

$$\psi_{\alpha,\beta} : \mathbb{Z}^{2n} \to S_{\alpha,\beta}$$

taking the first n standard generators of $\mathbb{Z}^{2n}$ to the classes $[\alpha_i], i = 1, \dots, n$, and the remaining n standard generators to the classes $[\beta_i], i = 1, \dots, n$. There is a short exact sequence

$$0 \longrightarrow \mathbb{Z} \longrightarrow \Pi_{\alpha,\beta} \longrightarrow \ker(\psi_{\alpha,\beta}) \longrightarrow 0. \tag{5}$$

Indeed, the map $\Pi_{\alpha,\beta} \to \ker(\psi_{\alpha,\beta})$ takes a periodic domain $\mathcal{D}$ to the coefficients of the alpha and beta curves appearing in $\partial\mathcal{D}$. It is surjective, and its kernel is generated by the Heegaard surface Σ itself.

The conclusion follows immediately from the short exact sequence. □

Note that we can view Π_α and Π_β as subgroups of $\Pi_{\alpha,\beta}$. Their intersection is generated by the two-chain Σ. Therefore,

$$\mathrm{rank}(\Pi_\alpha + \Pi_\beta) = 2m - 1.$$

More precisely, if we denote by $S_\alpha \oplus S_\beta \cong \mathbb{Z}^{2g}$ the exterior direct sum, there is a short exact sequence analogous to (5):

$$0 \to \mathbb{Z} \longrightarrow \Pi_\alpha + \Pi_\beta \longrightarrow \ker(\mathbb{Z}^{2n} \to S_\alpha \oplus S_\beta) \to 0. \tag{6}$$

Corollary 7. *If $S_{\alpha,\beta} = H_1(\Sigma;\mathbb{Z})$, then $\Pi_{\alpha,\beta} = \Pi_\alpha + \Pi_\beta$.*

Proof. The exact sequences (5) and (6) fit into a commutative diagram

$$\begin{array}{ccccccccc}
0 & \longrightarrow & \mathbb{Z} & \longrightarrow & \Pi_\alpha + \Pi_\beta & \longrightarrow & \ker(\mathbb{Z}^{2n} \to S_\alpha \oplus S_\beta) & \longrightarrow & 0 \\
 & & \cong\downarrow & & \downarrow & & \downarrow & & \\
0 & \longrightarrow & \mathbb{Z} & \longrightarrow & \Pi_{\alpha,\beta} & \longrightarrow & \ker(\mathbb{Z}^{2n} \to S_{\alpha,\beta}) & \longrightarrow & 0
\end{array}$$

To show that the middle vertical arrow is an isomorphism it suffices to show that the right vertical arrow is. The map $\psi_{\alpha,\beta} : \mathbb{Z}^{2n} \to S_{\alpha,\beta}$ factors through $S_\alpha \oplus S_\beta$. Consider the sequence of maps

$$\mathbb{Z}^{2g} \cong S_\alpha \oplus S_\beta \longrightarrow S_{\alpha,\beta} \hookrightarrow H_1(\Sigma;\mathbb{Z}) \cong \mathbb{Z}^{2g}.$$

The hypothesis says that the last inclusion is an isomorphism, which means that the composition is surjective. Since its domain and target are both $\mathbb{Z}^{2g}$, the map must be an isomorphism. This shows that $S_\alpha \oplus S_\beta \longrightarrow S_{\alpha,\beta}$ is an isomorphism as well. □

Finally, a *triple Heegaard diagram* $(\Sigma, \boldsymbol{\alpha}, \boldsymbol{\beta}, \boldsymbol{\gamma})$ consists of a Riemann surface Σ together with three good collections of curves $\boldsymbol{\alpha} = (\alpha_1, \dots, \alpha_n), \boldsymbol{\beta} = (\beta_1, \dots, \beta_n), \boldsymbol{\gamma} = (\gamma_1, \dots, \gamma_n)$. A *triply periodic domain* is then a two-chain on Σ that is a linear combination of the components of $\Sigma - (\cup\alpha_i) - (\cup\beta_i) - (\cup\gamma_i)$, and with the property that its boundary is a linear combination of the alpha, beta, and gamma curves.

The group of triply periodic domains is denoted $\Pi_{\alpha,\beta,\gamma}$. Set $S_{\alpha,\beta,\gamma} = S_\alpha + S_\beta + S_\gamma \subset H_1(\Sigma;\mathbb{Z})$. A straightforward analog of Lemma 6 then says that $\Pi_{\alpha,\beta,\gamma}$ is a free Abelian group of rank equal to $3n + 1 - \mathrm{rank}(S_{\alpha,\beta,\gamma})$.

3.2. **The ungraded triangle.** The following theorem was proved in [9]:

Theorem 8. *Let L be a link in S^3, and L_0 and L_1 the two resolutions of L at a crossing, as in Figure 1. Denote by l, l_0, l_1 the number of components of the links L, L_0, and L_1, respectively, and set $m = \max\{l, l_0, l_1\}$. Then, there is an exact triangle*

$$\widehat{HFK}(L) \otimes V^{m-l} \to \widehat{HFK}(L_0) \otimes V^{m-l_0} \to \widehat{HFK}(L_1) \otimes V^{m-l_1} \to \widehat{HFK}(L) \otimes V^{m-l},$$

where V denotes a two-dimensional vector space over $\mathbb{F}$.

Our goal will be to study how the maps in the exact triangle behave with respect to the δ-grading. In order to do this, we recall how the maps were constructed in [9].

The starting point is a special Heegaard diagram which we associate to a regular, connected, planar projection D of the link L. (This is a suitable stabilization of the diagram considered in [16].) We assume that one of the crossings in D is c_0, such that the two resolutions at c_0 are diagrams D_0 and D_1 for L_0 and L_1, respectively. If D has k crossings, then it splits the plane into $k + 2$ regions. Let A_0, A_1, A_2, A_3 be the regions near c_0 in clockwise order, as in Figure 5, and e the edge separating A_0 from A_1. We can assume that A_0 is the unbounded region in $\mathbb{R}^2 - D$. Denote the remaining regions by $A_4, \dots, A_{k+1}$. Let p be a point on the edge e. If $m = \max\{l, l_0, l_1\}$ is as in the statement of Theorem 8, then we

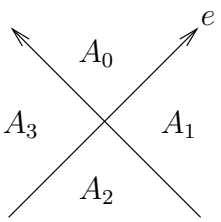

FIGURE 5. The regions near the crossing c_0. Since c_0 can be either negative or positive, we have not marked which strand is the overpass.

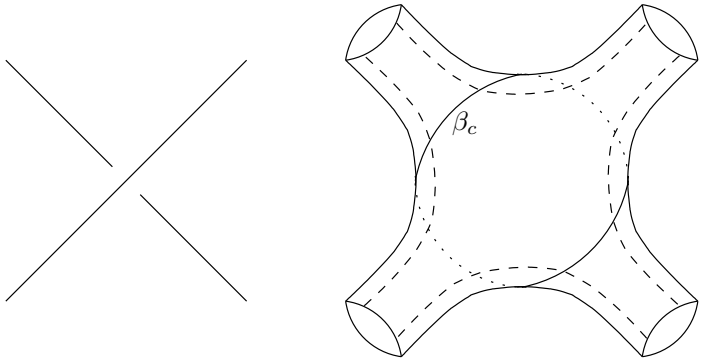

FIGURE 6. Piece of the Heegaard surface Σ associated to a crossing c. It contains four (or fewer) bits of alpha curves, shown in dashed lines, and one beta curve β_c.

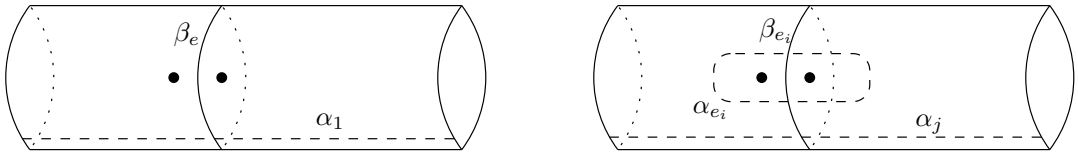

FIGURE 7. A neighborhood of the distinguished edge e (left) and a ladybug around some edge e_i marked by p_i (right).

can choose $p_1, \ldots, p_{m-1}$ to be a collection of points in the plane, distinct from the crossings and such that for every component of any of the links L, L_0 and L_1, the projection of that component contains at least one of the points p_i or p.

We denote by Σ the boundary of a regular neighborhood of D in S^3, a surface of genus $g = k + 1$. To every region A_r $(r > 0)$ we associate a curve α_r on Σ, following the boundary of A_r. To each crossing c in D we associate a curve β_c on Σ as indicated in Figure 6. In addition, we introduce an extra curve β_e which is the meridian of the knot, supported in a neighborhood of the distinguished edge e. We also mark the surface Σ with two basepoints, one on each side of β_e, as shown on the left side of Figure 7.

Furthermore, for every edge e_i of D containing one of the points p_i, $i = 1, \ldots, m-1$, we introduce a ladybug, i.e. an additional pair of alpha-beta curves on Σ, as well as an additional pair of basepoints. This type of configuration is shown on the right side of Figure 7.

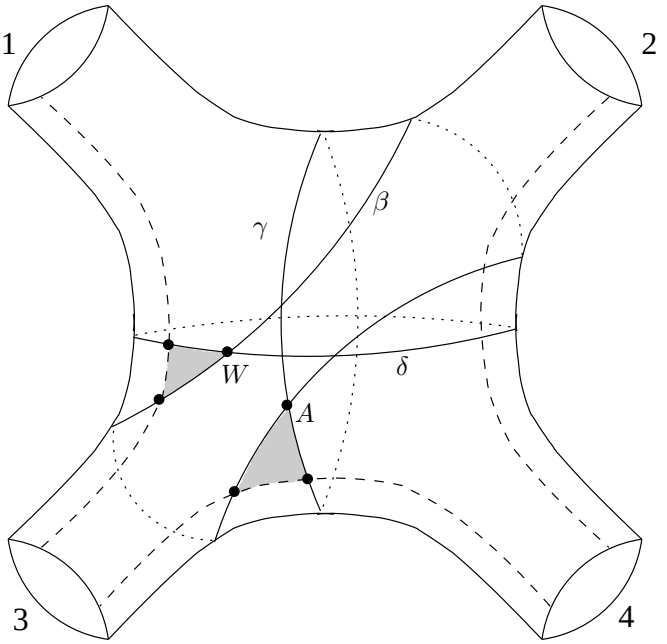

FIGURE 8. Piece of Σ near the crossing c_0. There are three bits of alpha curves, shown dashed. This piece is joined to the rest of the diagram by four tubes, which we mark by the numbers 1,2,3,4.

The surface Σ, together with the collections of alpha curves, beta curves and basepoints, forms a multi-pointed Heegaard diagram for S^3 compatible with L, in the sense of [10, Definition 2.1]. We denote the alpha and the beta curves in the diagram by α_i, β_i with $i = 1, \dots, n$, where $n = g + m - 1$. We reserve the index n for the beta curve $\beta = \beta_n$ associated to the crossing c_0. Also, we let $\widehat{\Sigma}$ denote the complement of the basepoints in the surface Σ.

We can construct similar Heegaard diagrams compatible with L_0 and L_1 as follows. The surface Σ, the alpha curves and the basepoints remain the same. However, for L_0 we replace the beta curves by gamma curves $\gamma_i,\ i = 1, \dots, n$, while for L_1 we use delta curves $\delta_i,\ i = 1, \dots, n$. For $i < n$, the curves γ_i and δ_i are small isotopic translates of β_i, such that they intersect β_i in two points, and they also intersect each other in two points. For $i = n$, we draw the curves $\gamma = \gamma_n$ and $\delta = \delta_n$ as in Figure 8; see also Figure 9, where the following intersection points are labelled:

$$\beta \cap \gamma = \{A, U\}, \quad \gamma \cap \delta = \{B, V\}, \quad \delta \cap \beta = \{C, W\}.$$

For the purpose of defining Floer homology, we need to ensure that the Heegaard diagrams for L, L_0 and L_1 constructed above are admissible in the sense of [22, Definition 3.5]. We achieve admissibility by stretching one tip of the alpha curve of each ladybug, and bringing it close to the basepoints associated to the distinguished edge e. It is easy to see that the result is admissible; see Figure 10 for an example. In that figure, to get the diagrams for L_0 and L_1, which are both the unknot, we replace $\beta = \beta_4$ by curves γ and δ, respectively, as in Figure 8.

Now consider the tori

$$\mathbb{T}_\alpha = \alpha_1 \times \cdots \times \alpha_n, \quad \mathbb{T}_\beta = \beta_1 \times \cdots \times \beta_n,$$

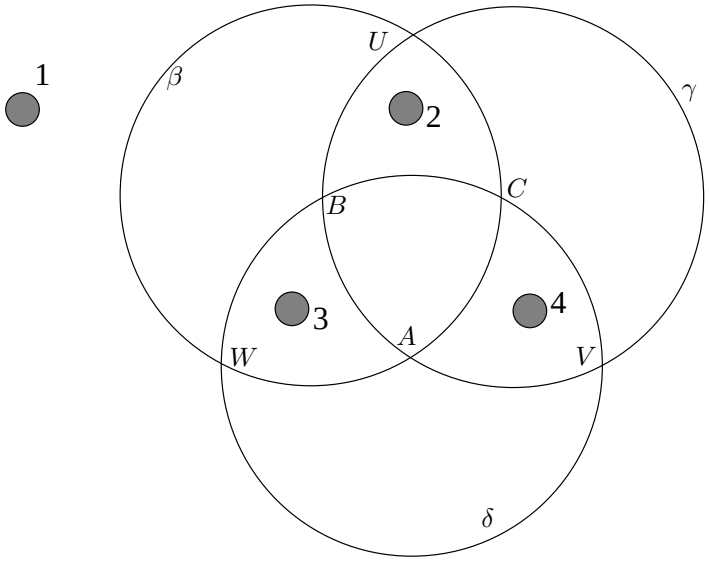

FIGURE 9. A different view of Figure 8. The four gray disks correspond to the four tubes from Figure 8, and are marked accordingly.

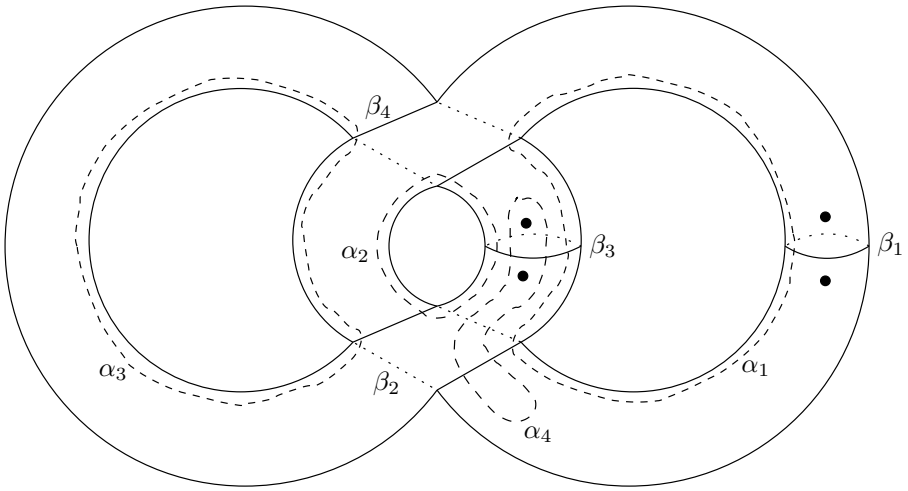

FIGURE 10. A Heegaard diagram compatible with the Hopf link L, with $g = 3, m = 2$ and $n = 4$. The beta curves β_2 and $\beta = \beta_4$ are associated to the two crossings, β_1 to the distinguished edge, and β_3 is part of a ladybug. There are three alpha curves associated to planar bounded regions and one, α_4, which is part of a ladybug. One tip of α_4 is stretched to achieve admissibility.

$$\mathbb{T}_\gamma = \gamma_1 \times \cdots \times \gamma_n, \quad \mathbb{T}_\delta = \delta_1 \times \cdots \times \delta_n,$$

which we view as totally real submanifolds of the symmetric product $\mathrm{Sym}^n(\widehat{\Sigma})$. The Floer complex $CF(\mathbb{T}_\alpha, \mathbb{T}_\beta)$ is the vector space freely generated by the intersection points between

$\mathbb{T}_\alpha$ and $\mathbb{T}_\beta$, and endowed with the differential

$$\partial \mathbf{x} = \sum_{\mathbf{y} \in \mathbb{T}_\alpha \cap \mathbb{T}_\beta} \sum_{\{\phi \in \hat{\pi}_2(\mathbf{x},\mathbf{y}) \,\big|\, \mu(\phi)=1\}} \#\left(\frac{\mathcal{M}(\phi)}{\mathbb{R}}\right) \mathbf{y}. \tag{7}$$

Here $\hat{\pi}_2(\mathbf{x},\mathbf{y})$ denotes the space of homology classes of Whitney disks connecting $\mathbf{x}$ to $\mathbf{y}$ in $\mathrm{Sym}^n(\widehat{\Sigma})$, $\mathcal{M}(\phi)$ denotes the moduli space of pseudo-holomorphic representatives of ϕ (with respect to a suitable almost complex structure as in [18]), $\mu(\phi)$ denotes its formal dimension (Maslov index), and the # sign denotes the mod 2 count of points in the (zero-dimensional) moduli space. (We will henceforth use μ to denote Maslov index, rather than the incidence number, as in Section 2.)

The homology of $CF(\mathbb{T}_\alpha, \mathbb{T}_\beta)$ is the Floer homology $HF(\mathbb{T}_\alpha, \mathbb{T}_\beta)$. Up to a factor, this is the knot Floer homology of L:

$$HF(\mathbb{T}_\alpha, \mathbb{T}_\beta) \cong \widehat{HFK}(L) \otimes V^{m-l},$$

where V is a two-dimensional vector space as in Theorem 8.

We can similarly take the Floer homology of $\mathbb{T}_\alpha$ and $\mathbb{T}_\gamma$, or $\mathbb{T}_\alpha$ and $\mathbb{T}_\delta$, and obtain

$$HF(\mathbb{T}_\alpha, \mathbb{T}_\gamma) \cong \widehat{HFK}(L_0) \otimes V^{m-l_0},$$

$$HF(\mathbb{T}_\alpha, \mathbb{T}_\delta) \cong \widehat{HFK}(L_1) \otimes V^{m-l_1}.$$

Therefore, the exact triangle from Theorem 8 can be written as

$$HF(\mathbb{T}_\alpha, \mathbb{T}_\delta) \xrightarrow{(f_1)_*} HF(\mathbb{T}_\alpha, \mathbb{T}_\beta) \xrightarrow{(f_2)_*} HF(\mathbb{T}_\alpha, \mathbb{T}_\gamma) \xrightarrow{(f_3)_*} HF(\mathbb{T}_\alpha, \mathbb{T}_\delta) \tag{8}$$

The maps $(f_i)_*$ $(i = 1, 2, 3)$ from the triangle (8) are all induced by chain maps f_i between the corresponding Floer complexes. To define the maps f_i, let us first recall the definition of the usual triangle maps appearing in Floer theory. Given totally real submanifolds T_1, T_2, T_3 in a symplectic manifold (satisfying several technical conditions which will hold in our situations), there is a chain map

$$CF(T_1, T_2) \otimes CF(T_2, T_3) \to CF(T_1, T_3),$$

defined by counting pseudo-holomorphic triangles. In particular, given an intersection point $\mathbf{z} \in T_2 \cap T_3$ which is a cycle when viewed as an element of $CF(T_2, T_3)$, we have a chain map

$$F_{\mathbf{z}}(\mathbf{x}) = \sum_{\mathbf{y} \in T_1 \cap T_3} \sum_{\{\phi \in \hat{\pi}_2(\mathbf{x},\mathbf{z},\mathbf{y}) \,\big|\, \mu(\phi)=0\}} \#\left(\mathcal{M}(\phi)\right) \mathbf{y}.$$

Here $\hat{\pi}_2(\mathbf{x},\mathbf{z},\mathbf{y})$ denotes the space of homology classes of triangles with edges on T_1, T_2, T_3 and vertices $\mathbf{x}, \mathbf{z}$ and $\mathbf{y}$, respectively (in clockwise order), μ is the Maslov index, and $\#\left(\mathcal{M}(\phi)\right)$ the number of their pseudo-holomorphic representatives.

Going back to our set-up, whenever we have two isotopic curves η and η' on the surface Σ such that they intersect in exactly two points, we will denote by $M_{\eta\eta'} \in \eta \cap \eta'$ the top degree generator of $CF(\eta, \eta')$. Given one of the intersection points in Figure 9, for example $A \in \beta \cap \gamma$, we obtain a corresponding intersection point in $\mathbb{T}_\beta \cap \mathbb{T}_\gamma$ by adjoining to A the top degree intersection points $M_{\beta_i\gamma_i} \in \beta_i \cap \gamma_i$. We denote the resulting generators by the respective lowercase letters in bold:

$$\mathbf{a} = M_{\beta_1\gamma_1} \times M_{\beta_2\gamma_2} \times \cdots \times M_{\beta_{n-1}\gamma_{n-1}} \times A \in \mathbb{T}_\beta \cap \mathbb{T}_\gamma;$$

$$\mathbf{b} = M_{\gamma_1\delta_1} \times M_{\gamma_2\delta_2} \times \cdots \times M_{\gamma_{n-1}\delta_{n-1}} \times B \in \mathbb{T}_\gamma \cap \mathbb{T}_\delta;$$

$$\mathbf{c} = M_{\delta_1\beta_1} \times M_{\delta_2\beta_2} \times \cdots \times M_{\delta_{n-1}\beta_{n-1}} \times C \in \mathbb{T}_\delta \cap \mathbb{T}_\beta;$$

$$\mathbf{u} = M_{\beta_1\gamma_1} \times M_{\beta_2\gamma_2} \times \cdots \times M_{\beta_{n-1}\gamma_{n-1}} \times U \in \mathbb{T}_\beta \cap \mathbb{T}_\gamma;$$
$$\mathbf{v} = M_{\gamma_1\delta_1} \times M_{\gamma_2\delta_2} \times \cdots \times M_{\gamma_{n-1}\delta_{n-1}} \times V \in \mathbb{T}_\gamma \cap \mathbb{T}_\delta;$$
$$\mathbf{w} = M_{\delta_1\beta_1} \times M_{\delta_2\beta_2} \times \cdots \times M_{\delta_{n-1}\beta_{n-1}} \times W \in \mathbb{T}_\delta \cap \mathbb{T}_\beta.$$

The chain maps f_i giving rise to (8) are then defined to be the sums

$$f_1 = F_{\mathbf{c}} + F_{\mathbf{w}} : CF(\mathbb{T}_\alpha, \mathbb{T}_\delta) \to CF(\mathbb{T}_\alpha, \mathbb{T}_\beta);$$
$$f_2 = F_{\mathbf{a}} + F_{\mathbf{u}} : CF(\mathbb{T}_\alpha, \mathbb{T}_\beta) \to CF(\mathbb{T}_\alpha, \mathbb{T}_\gamma);$$
$$f_3 = F_{\mathbf{b}} + F_{\mathbf{v}} : CF(\mathbb{T}_\alpha, \mathbb{T}_\gamma) \to CF(\mathbb{T}_\alpha, \mathbb{T}_\delta).$$

3.3. **Periodic domains.** Let us apply the discussion in Section 3.1 to the setting of Section 3.2.

Note that $(\Sigma; \boldsymbol{\alpha}, \boldsymbol{\beta})$, for example, is a Heegaard diagram for S^3, hence the alpha and the beta curves span all of $H_1(\Sigma; \mathbb{Z})$. Applying Corollary 7 we deduce that

$$\Pi_{\alpha,\beta} = \Pi_\alpha + \Pi_\beta. \tag{9}$$

Similarly, we have $\Pi_{\alpha,\gamma} = \Pi_\alpha + \Pi_\gamma$ and $\Pi_{\alpha,\delta} = \Pi_\alpha + \Pi_\delta$.

The situation for $\Pi_{\beta,\gamma}$ is different. Before analyzing it, let us first understand the components of $\Sigma - (\cup\beta_i)$, which span Π_β, in detail. Their number is m, which equals either l or $l+1$, according to whether the two strands of L meeting at c are on different link components, or on the same link component. Let $K_1, \ldots, K_l$ be the connected components of L, such that K_l is the one containing the edge e. If $m = l$, then each K_i corresponds to a unique component $\mathcal{D}_i^\beta$ of $\Sigma - (\cup\beta_i)$, which lies in a neighborhood of K_i (when Σ is viewed as the boundary of a neighborhood of L). If $m = l+1$, then for $i < l$, each K_i corresponds again to some $\mathcal{D}_i^\beta$, but in the neighborhood of K_l there are now two components of $\Sigma - (\cup\beta_i)$, which we denote by $\mathcal{D}_l^\beta$ and $\mathcal{D}_{l+1}^\beta$, such that $\mathcal{D}_l^\beta$ is the one whose boundary contains the curve $\beta = \beta_n$.

Note that, regardless of whether $m = l$ or $m = l+1$, the component $\mathcal{D}_l^\beta$ contains the curve β_n with multiplicity ± 1 (see Figure 3.3). This means that the class $[\beta_n] \in S_\beta \subset H_1(\Sigma; \mathbb{Z})$ is in the span of the other beta curves. In other words,

$$S_\beta = \text{ Span } (\beta_1, \ldots, \beta_{n-1}). \tag{10}$$

Similar remarks apply to $\Sigma - (\cup\gamma_i)$ and $\Sigma - (\cup\delta_i)$. Their components are denoted $\mathcal{D}_i^\gamma$ and $\mathcal{D}_i^\delta$, respectively, for $i = 1, \ldots, m$. Recall that for each $i = 1, \ldots, n-1$, the curves β_i, γ_i and δ_i are isotopic. Therefore, Equation (10), together with its analogs for the beta and gamma curves, implies that

$$S_\beta = S_\gamma = S_\delta. \tag{11}$$

For each $j = 1, \ldots, n-1$, the curves β_j and γ_j are separated by two thin bigons in Σ. The difference of these bigons is a periodic domain $\mathcal{D}_j^{\beta,\gamma}$, with boundary $\beta_j - \gamma_j$. Equation (11) implies that $\text{rank}(S_{\beta,\gamma}) = \text{rank}(S_\beta) = g$, so from Lemma 6 we deduce that $\text{rank}(\Pi_{\beta,\gamma}) = 2n + 1 - g = n + m$. In fact, it is not hard to check that the following is true:

Lemma 9. *The domains $\mathcal{D}_i^\beta, \mathcal{D}_i^\gamma$ $(i = 1, \ldots, m)$ and $\mathcal{D}_j^{\beta,\gamma}$ $(j = 1, \ldots, n-1)$ span the group $\Pi_{\beta,\gamma}$.*

Note that we gave a set of $2m + n - 1$ generators for the group $\Pi_{\beta,\gamma}$ of rank $n + m$. There are indeed $m - 1$ indpendent relations between these generators, namely for each of the $m - 1$ components K_i of L (or L_0) not containing either of the strands intersecting at c,

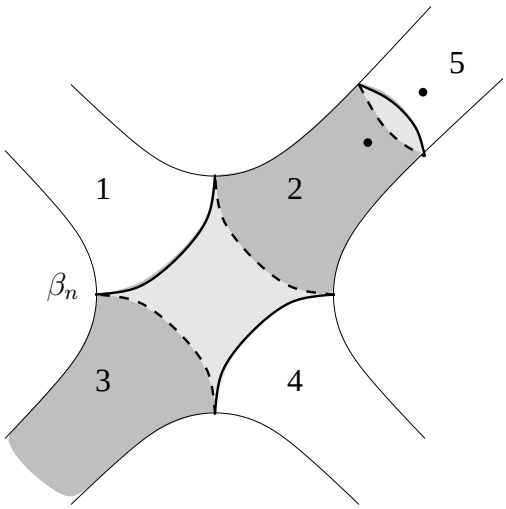

FIGURE 11. We illustrate here Equation (10). The component $\mathcal{D}_l^\beta$, which gives a homological relation between β_n and other β-curves, is shaded. There are two cases: when $m = \ell$, the region labelled here by 5 is included in $\mathcal{D}_l^\beta$. Otherwise, when $m = \ell + 1$, $\mathcal{D}_l^\beta$ terminates in a different meridinal β-circle. In either case, the boundary of $\mathcal{D}_l^\beta$ consists of β-circles, and it contains β_n with multiplicity one.

the difference $\mathcal{D}_i^\beta - \mathcal{D}_i^\gamma$ can also be written as a sum of some domains $\mathcal{D}_j^{\beta,\gamma}$ (corresponding to the crossings on K_i).

Next, let us look at the triply periodic domains with boundary on the alpha, beta, and gamma curves.

Lemma 10. *We have* $\Pi_{\alpha,\beta,\gamma} = \Pi_\alpha + \Pi_{\beta,\gamma}$.

Proof. Let $\mathcal{D}$ be any triply periodic domain in $\Pi_{\alpha,\beta,\gamma}$. If the curve γ_n appears (with nonzero multiplicity) in the boundary of $\mathcal{D}$, by the analog of (10) for gamma curves we can subtract some domain in $\Pi_\gamma \subset \Pi_{\beta,\gamma}$ from $\mathcal{D}$ and obtain a new domain, in which the multiple of γ_n from $\partial\mathcal{D}$ was traded for a combination of the other gamma curves $\gamma_1, \dots, \gamma_{n-1}$. Next, whenever we have some curve γ_j in the boundary ($j < n$), we can add the corresponding domain $\mathcal{D}_j^{\beta,\gamma} \in \Pi_\beta \subset \Pi_{\beta,\gamma}$ to trade it for a beta curve. Thus we arrive at a domain in $\Pi_{\alpha,\beta}$ and the conclusion follows from Equation (9). □

Note that Lemma 9 has straightforward analogs about the structure of the groups $\Pi_{\gamma,\delta}$ and $\Pi_{\delta,\beta}$. Similarly, Lemma 10 has straightforward analogs about the structure of the groups $\Pi_{\alpha,\gamma,\delta}$ and $\Pi_{\alpha,\delta,\beta}$.

3.4. **The relative δ-grading.** Pick $\mathbf{x}, \mathbf{y} \in \mathbb{T}_\alpha \cap \mathbb{T}_\beta$. Let $\pi_2(\mathbf{x}, \mathbf{y})$ be the space of homology classes of Whitney disks in $\mathrm{Sym}^n(\Sigma)$ connecting $\mathbf{x}$ and $\mathbf{y}$. (Recall that $\hat{\pi}_2(\mathbf{x}, \mathbf{y})$ is the corresponding space in $\mathrm{Sym}^n(\widehat{\Sigma})$.) Since $(\Sigma, \alpha_1, \dots, \alpha_n, \beta_1, \dots, \beta_n)$ is a Heegaard diagram for S^3, we have $\pi_2(\mathbf{x}, \mathbf{y}) \neq \emptyset$ for any $\mathbf{x}$ and $\mathbf{y}$. Note that $\pi_2(\mathbf{x}, \mathbf{x})$ can be identified with the group of periodic domains $\Pi_{\alpha,\beta}$.

Every class $\phi \in \pi_2(\mathbf{x}, \mathbf{y})$ has a Maslov index $\mu(\phi) \in \mathbb{Z}$. In the usual construction of knot Floer homology, the extra basepoints on the Heegaard surface Σ are of two types: half of them are denoted w_j and the other half z_j, with $j = 1, \cdots, m+1$, such that every connected

component of $\Sigma - \cup\alpha_i$ or $\Sigma - \cup\beta_i$ contains exactly one of the w_j and one of the z_k. Let $W(\phi)$ and $Z(\phi)$ be the intersection numbers of ϕ with the union of all $\{w_j\} \times \mathrm{Sym}^{n-1}(\Sigma)$ and the union of all $\{z_j\} \times \mathrm{Sym}^{n-1}(\Sigma)$, respectively. Thus $\hat{\pi}_2(\mathbf{x}, \mathbf{y})$ is the space of classes ϕ with $W(\phi) = Z(\phi) = 0$.

The difference in the Maslov grading H (denoted i in the introduction) between $\mathbf{x}$ and $\mathbf{y}$ can be calculated by picking some $\phi \in \pi_2(\mathbf{x}, \mathbf{y})$ and applying the formula

$$H(\mathbf{x}) - H(\mathbf{y}) = \mu(\phi) - 2W(\phi).$$

Similarly, the difference in the Alexander grading A (denoted j in the introduction) is

$$A(\mathbf{x}) - A(\mathbf{y}) = Z(\phi) - W(\phi).$$

Setting $P(\phi) = Z(\phi) + W(\phi)$, the difference in the grading $\delta = A - H$ is then

$$\delta(\mathbf{x}) - \delta(\mathbf{y}) = P(\phi) - \mu(\phi).$$

Therefore, if we limit ourselves to considering the δ grading, there is no difference between the two types of basepoints. This explains why we have not distinguished between them in Section 3.2, and we will not distinguish between them from now on either.

Observe that the relative δ grading is well-defined, i.e. we have $\mu(\phi) - P(\phi) = \mu(\phi') - P(\phi')$ for any $\phi, \phi' \in \pi_2(\mathbf{x}, \mathbf{y})$. Indeed, because μ and P are additive under concatenation, it suffices to prove that $\mu(\phi) - P(\phi) = 0$ for any $\phi \in \pi_2(\mathbf{x}, \mathbf{x}) = \Pi_{\alpha\beta}$. By Equation (9), the group $\Pi_{\alpha\beta}$ is generated by the connected components of $\Sigma - \cup\alpha_i$ and $\Sigma - \cup\beta_i$. Each such component has $\mu(\phi) = P(\phi) = 2$, so the relative δ grading is well-defined.

Lemma 11. *The chain maps f_1, f_2, f_3 that induce the triangle* (8) *preserve the relative δ grading.*

Proof. First, observe that a triangle map such as $F_{\mathbf{a}} : CF(\mathbb{T}_\alpha, \mathbb{T}_\beta) \to CF(\mathbb{T}_\alpha, \mathbb{T}_\gamma)$ preserves the relative δ grading. In other words, we need to show that adding a triply periodic domain $\mathcal{D} \in \Pi_{\alpha,\beta,\gamma}$ to a class $\phi \in \hat{\pi}_2(\mathbf{x}, \mathbb{Z}, \mathbf{y})$ does not change the quantity $\mu(\phi) - P(\phi)$. By Lemmas 9 and 10, it suffices to show that the classes of the domains $\mathcal{D}_i^\alpha, \mathcal{D}_i^\beta, \mathcal{D}_i^\gamma$ and $\mathcal{D}_j^{\beta,\gamma}$ all have $\mu = P$. Indeed, for $\mathcal{D}_i^\alpha, \mathcal{D}_i^\beta$ and $\mathcal{D}_i^\gamma$ this is the argument in the paragraph before Lemma 11, while for each $\mathcal{D}_j^{\beta,\gamma}$ $(j = 1, \ldots, n-1)$ we have $\phi = P = 0$.

Next, in order to show that $f_2 = F_{\mathbf{a}} + F_{\mathbf{u}}$ preserves the relative δ-grading, we exhibit a class $\phi \in \pi_2(\mathbf{a}, \mathbf{u})$ with $\mu(\phi) = P(\phi)$. In Figure 9 there is a bigon relating A and U which is connected by the tube numbered 2 to the rest of the Heegaard diagram. This bigon is also shown on the left in Figure 12. Following the tube, we encounter several disks (or possibly none) bounded by beta circles as in the middle of Figure 12, until we find a disk as on the right of Figure 12. Lipshitz's formula for the Maslov index [8] says that $\mu(\phi)$ can be computed as the sum of the Euler measure $e(\phi)$ and a vertex multiplicity $n(\phi)$. (We refer to [8] for the definitions.) The punctured bigon on the left of Figure 12 contributes $-\frac{1}{2}$ to $e(\phi)$ and $\frac{1}{2}$ to $n(\phi)$, each middle disk -1 to $e(\phi)$ and 1 to $n(\phi)$, and the disk on the right 0 to $e(\phi)$ and 1 to $n(\phi)$. Thus $\mu(\phi) = P(\phi) = 1$.

The arguments for f_1 and f_3 are similar. □

3.5. **The absolute δ-grading.** The generators $\mathbf{x} \in \mathbb{T}_\alpha \cap \mathbb{T}_\beta$ are of two kinds. They all consist of n-tuples of points in Σ, one on each alpha curve and on each beta curve. If for each ladybug (consisting of a pair of curves α_i and β_i), $\mathbf{x}$ contains one of the two points in $\alpha_i \cap \beta_i$, we call the generator $\mathbf{x}$ *Kauffman*. Otherwise, it is called *non-Kauffman*. Note that, if we hadn't had to stretch the alpha curves on the ladybugs to achieve admissibility, all generators would have been Kauffman.

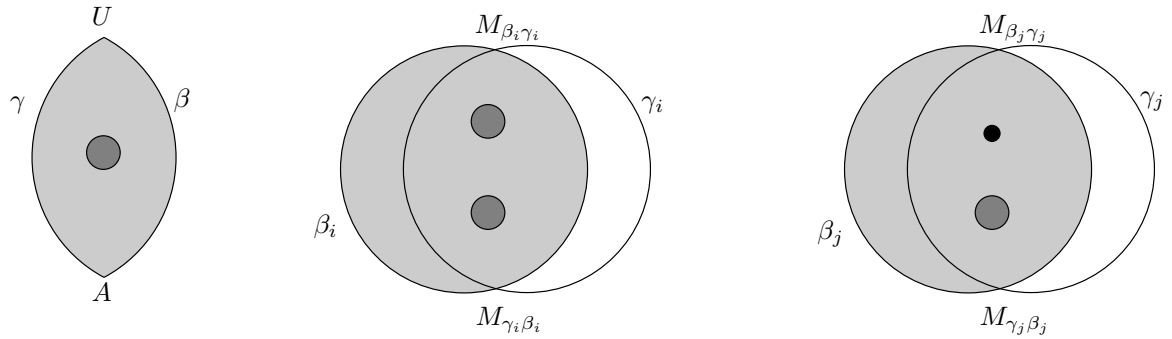

FIGURE 12. A relative homology class $\phi \in \pi_2(\mathbf{a}, \mathbf{u})$ of Maslov index 1, with one basepoint. The grey disks here denote tubes, whereas the small black dot in the rightmost picture denotes a basepoint.

FIGURE 13. Contributions to the δ-grading.

Every $\mathbf{x} \in \mathbb{T}_\alpha \cap \mathbb{T}_\beta$ has an absolute δ-grading $\delta(\mathbf{x}) \in \frac{1}{2}\mathbb{Z}$. We will explain now a simple formula for $\delta(\mathbf{x})$ when $\mathbf{x}$ is Kauffman.

Consider the regions $A_0, A_1, A_2, \dots, A_{k+1}$ as in the second paragraph after the statement of Theorem 8. Each of the k crossings in D is on the boundary of four regions. A *state*, cf. [4], is an assignment which associates to each crossing one of the four incoming quadrants, such that the quadrants associated to distinct vertices are in distinct regions, and none are corners of the regions A_0 or A_1.

One can associate a monomial to each state such that as we sum all these monomials we obtain the Alexander polynomial of the link L, [4]. Therefore, if the Alexander polynomial $\Delta_L(q)$ is nonzero (or, in particular, if $\Delta_L(-1) = \det(L) \neq 0$), then there must be at least one state.

To each Kauffman generator $\mathbf{x}$ we can associate a state in an natural way: at each crossing c the corresponding beta curve intersects exactly one of the alpha curves of the neighboring regions in a point of $\mathbf{x}$, and the quadrant in that region is the one we associate to c. In [16], the Maslov and Alexander gradings of Kauffman generators are calculated in terms of their states; compare also [14].

For our purposes, it suffices to know how to compute the δ-grading. If $\mathbf{x}$ is Kauffman and c is a crossing in D, we let $\delta(\mathbf{x}, c) \in \{0, \pm 1/2\}$ be the quantity from Figure 13, chosen according to which quadrant at c appears in the state of $\mathbf{x}$. Then:

$$\delta(\mathbf{x}) = \sum_c \delta(\mathbf{x}, c). \tag{12}$$

A similar discussion applies to the diagrams D_0 and D_1 of the resolutions L_0 and L_1, respectively, except that in those cases there is no contribution from the resolved crossing c_0.

Note that the δ-grading of a Kauffman generator $\mathbf{x}$ does not depend on which of the two intersection points between the two curves of a ladybug appears in $\mathbf{x}$.

Lemma 12. *Suppose that c_0 is a positive crossing in D (so that L_0 is the oriented resolution L_v) and that $\det(L_0) \neq 0$. Then the map $f_2 : CF(\mathbb{T}_\alpha, \mathbb{T}_\beta) \to CF(\mathbb{T}_\alpha, \mathbb{T}_\gamma)$ decreases δ-grading by $1/2$.*

Proof. By Lemma 11, we already know that f_2 preserves the relative δ-grading. Thus, it suffices to exhibit two generators $\mathbf{x} \in \mathbb{T}_\alpha \cap \mathbb{T}_\beta$ and $\mathbf{y} \in \mathbb{T}_\alpha \cap \mathbb{T}_\gamma$ with $\delta(\mathbf{x}) - \delta(\mathbf{y}) = 1/2$, and such that there exists a holomorphic triangle of index zero in $\hat{\pi}_2(\mathbf{x}, \mathbf{a}, \mathbf{y})$.

Since $\det(L_0) \neq 0$, the diagram D_0 has at least one Kauffman generator $\mathbf{y}$. There is a corresponding Kauffman generator $\mathbf{x} \in \mathbb{T}_\alpha \cap \mathbb{T}_\beta$, such that each $y_i \in \gamma_i \cap \mathbf{y}$, $(i < n)$ is close to some $x_i \in \beta_i \cap \mathbf{x}$ (they are related by the isotopy between γ_i and β_i), while $x_n \in \beta \cap \mathbf{x}$ and $y_n \in \gamma \cap \mathbf{y}$ are two vertices of the shaded triangle in Figure 8 with the third vertex at A. That shaded triangle, coupled with the small triangles with vertices at $\mathbf{x}_i, \mathbf{y}_i$, and M_{β_i,γ_i} for $i = 1, \ldots, n-1$, gives the desired holomorphic triangle in $\mathrm{Sym}^n(\widehat{\Sigma})$. To check that $\delta(\mathbf{x}) - \delta(\mathbf{y}) = 1/2$, note that in formula (12) the contributions to $\delta(\mathbf{x})$ and $\delta(\mathbf{y})$ from each crossing are the same, except that there is an extra contribution of $1/2$ to $\delta(\mathbf{x})$ coming from c_0. □

Lemma 13. *Suppose that c_0 is a positive crossing in D (so that L_1 is the unoriented resolution L_h) and that $\det(L_1) \neq 0$. Then the map $f_1 : CF(\mathbb{T}_\alpha, \mathbb{T}_\delta) \to CF(\mathbb{T}_\alpha, \mathbb{T}_\beta)$ shifts δ-grading by $e/2$, where e is as in the statement of Lemma 3.*

Proof. By Lemma 11, we already know that f_1 preserves the relative δ-grading. Again, it suffices to exhibit two generators $\mathbf{x} \in \mathbb{T}_\alpha \cap \mathbb{T}_\beta$ and $\mathbf{y} \in \mathbb{T}_\alpha \cap \mathbb{T}_\delta$ with $\delta(\mathbf{x}) - \delta(\mathbf{y}) = e/2$, and such that there exists a holomorphic triangle of index zero in $\hat{\pi}_2(\mathbf{y}, \mathbf{w}, \mathbf{x})$.

Since $\det(L_1) \neq 0$, we can pick a Kauffman generator $\mathbf{y} \in \mathbb{T}_\alpha \cap \mathbb{T}_\delta$. As in the proof of Lemma 12, there is a corresponding Kauffman generator $\mathbf{x} \in \mathbb{T}_\alpha \cap \mathbb{T}_\beta$ and a holomorphic triangle of index zero as desired, consisting of $n-1$ small triangles with one vertex at M_{δ_i,β_i} for $i = 1, \ldots, n-1$, and the shaded triangle in Figure 8 with one vertex at W.

To check that $\delta(\mathbf{x}) - \delta(\mathbf{y}) = e/2$, let n_+ be the number of positive crossings in D (excluding c_0) which change sign in D_1. At each such crossing c, we have:

$$\delta(\mathbf{x}, c) = \delta(\mathbf{y}, c) + 1/2.$$

Let also n_- be the number of negative crossings in D which change sign in D_1. At each such crossing c, we have:

$$\delta(\mathbf{x}, c) = \delta(\mathbf{y}, c) - 1/2.$$

Therefore,

$$\delta(\mathbf{x}) - \delta(\mathbf{y}) = (n_+ - n_-)/2 = e/2.$$

□

Proposition 14. *Let L be a link and L_0, L_1 its two resolutions at a crossing as in Figure 1. Assume that $\det(L_0), \det(L_1) > 0$ and $\det(L) = \det(L_0) + \det(L_1)$. Then, with respect to the δ-grading, the exact triangle from Theorem 8 can be written as*

$$\widehat{HFK}_{*-\frac{\sigma(L_1)}{2}}(L_1) \otimes V^{m-l_1} \to \widehat{HFK}_{*-\frac{\sigma(L)}{2}}(L) \otimes V^{m-l_0} \to \widehat{HFK}_{*-\frac{\sigma(L_0)}{2}}(L_0) \otimes V^{m-l},$$

where V denotes a two-dimensional vector space over $\mathbb{F}$, in grading zero.

Proof. When the given crossing in L is positive, this follows from (8), together with the results of Lemmas 3, 12, and 13. The case when the crossing is negative is similar. □

Proof of Theorem 2. Using Proposition 14, we can argue in the same way as in the proof of Theorem 1. Note that we do not have to know the change in the absolute δ-grading under the map $(f_3)_* : HF(\mathbb{T}_\alpha, \mathbb{T}_\gamma) \to HF(\mathbb{T}_\alpha, \mathbb{T}_\delta)$ in the exact triangle. Indeed, recall that the Euler characteristic of $\widehat{HFK}$ is (up to a factor) the Alexander polynomial, which evaluated at -1 gives the determinant of the link. If we know that L_0 and L_1 are Floer homologically σ-thin and we want to show the same for L, the fact that $\det(L) = \det(L_0) + \det(L_1)$ together with the ungraded triangle implies that

$$\text{rank } (\widehat{HFK}(L) \otimes V^{m-l}) = \text{rank } (\widehat{HFK}(L_0) \otimes V^{m-l_0}) + \text{rank } (\widehat{HFK}(L_1) \otimes V^{m-l_1}).$$

Hence $(f_3)_* = 0$, and the inductive step goes through. □

References

[1] J. Baldwin, *Quasi-alternating 3-braid links*, in preparation.
[2] D. Bar-Natan, *On Khovanov's categorification of the Jones polynomial,* Alg. Geom. Top. **2** (2002), 337-370.
[3] C. Gordon and R. Litherland, *On the signature of a link,* Invent. Math. **47** (1978), 53-69.
[4] L. H. Kauffman, *Formal knot theory*, Mathematical Notes **30**, Princeton University Press (1983).
[5] M. Khovanov, *A categorification of the Jones polynomial,* Duke Math. J. **101** (2000), no. 3, 359-426.
[6] M. Khovanov, *Patterns in knot cohomology I,* Experiment. Math. **12** (2003), no. 3, 365–374.
[7] E. S. Lee, *The support of the Khovanov's invariants for alternating knots,* preprint(2002), math/0201105.
[8] R. Lipshitz, *A cylindrical reformulation of Heegaard Floer homology,* Geom. Topol. **10** (2006), 955–1097.
[9] C. Manolescu, *An unoriented skein exact triangle for knot Floer homology,* math/0609531, Math. Res. Lett., to appear.
[10] C. Manolescu, P. Ozsváth and S. Sarkar, *A combinatorial description of knot Floer homology,* preprint (2006), math/0607691.
[11] C. Manolescu, P. Ozsváth, Z. Szabó and D. Thurston, *On combinatorial link Floer homology,* math/0610559, Geom. Topol., to appear.
[12] K. Murasugi,*On a certain numerical invariant of link types,* Trans. Amer. Math. Soc. **117** (1965), 387–422.
[13] K. Murasugi, *On the signature of links,* Topology **9** (1970), 283–298.
[14] P. Ozsváth, A. Stipsicz, and Z. Szabó *Floer homology and singular knots*, preprint (2007), math/0705.2661.
[15] P. Ozsváth and Z. Szabó, *Holomorphic disks and knot invariants,* Adv. Math. **186** (2004), no. 1, 58–116.
[16] P. Ozsváth and Z. Szabó, *Heegaard Floer homology and alternating knots,* Geom. Topol. **7** (2003), 225–254.
[17] P. Ozsváth and Z. Szabó, *Holomorphic disks and genus bounds,* Geom. Topol. **8** (2004), 311–334 .
[18] P. Ozsváth and Z. Szabó, *Holomorphic disks and topological invariants for closed three-manifolds*, Ann. of Math. (2) **159** (2004), no. 3, 1027–1158.
[19] P. Ozsváth and Z. Szabó, *On the Heegaard Floer homology of branched double-covers,* Adv. Math. **194** (2005), 1-33.
[20] P. Ozsváth and Z. Szabó, *Knot Floer homology and integer surgeries,* preprint (2004), math/0410300.
[21] P. Ozsváth and Z. Szabó, *Knot Floer homology and rational surgeries,* preprint (2005), math/0504404.
[22] P. Ozsváth and Z. Szabó, *Holomorphic disks and link invariants,* preprint (2005), math/0512286.
[23] P. Ozsváth and Z. Szabó, *Link Floer homology and the Thurston norm,* preprint (2006), math/0601618.
[24] P. Ozsváth and Z. Szabó, *A cube of resolutions for knot Floer homology,* preprint (2007), math/0705.3852.
[25] Y. Ni, *Knot Floer homology detects fibred knots,* preprint (2006), math.GT/0607156.
[26] J. Rasmussen, *Floer homology of surgeries on two-bridge knots,* Alg. Geom. Top. **2** (2002), 757-789.
[27] J. Rasmussen, *Floer homology and knot complements,* Ph. D. Thesis, Harvard University (2003), math/0306378.

[28] J. Rasmussen, "Knot polynomials and knot homologies," in *Geometry and topology of manifolds,* 261–280, Fields Inst. Commun. **47**, Amer. Math. Soc., Providence, 200
[29] S. Sarkar and J. Wang, *A combinatorial description of some Heegaard Floer homologies,* preprint (2006), math/0607777.
[30] O. Viro, *Remarks on the definition of the Khovanov homology*, preprint (2002), math/0202199.

Department of Mathematics, Columbia University, New York, NY 10027
E-mail address: cm@math.columbia.edu

Department of Mathematics, Columbia University, New York, NY 10027
E-mail address: petero@math.columbia.edu